Published by IOP Publishing for SISSA
Received: *August 30, 2008*
Revised: *November 21, 2008*
Accepted: *December 5, 2008*
Published: *December 16, 2008*

Comment on 'A collider signature of the supersymmetric golden region'

Won Sang Cho, Yeong Gyun Kim and Chan Beom Park

Department of Physics, KAIST,
Daejeon 305-701, Korea
E-mail: wscho@muon.kaist.ac.kr, ygkim@muon.kaist.ac.kr, lunacy@muon.kaist.ac.kr

Abstract: We show that Z polarization measurement is useful for distinguishing the signal decay chain of the 'golden region' [1] in the minimal supersymmetric standard model(MSSM) parameter space, which involves the stop decay of $\tilde{t}_2 \to \tilde{t}_1 + Z$, from other decay chains involving the neutralino decay of $\tilde{\chi}_2^0 \to \tilde{\chi}_1^0 + Z$ in different MSSM scenarios. Within a given decay chain, Z polarization can also serve as an indicator of the mass difference of stops or neutralinos.

Keywords: Phenomenological Models, Supersymmetry Phenomenology.

JHEP12(2008)074

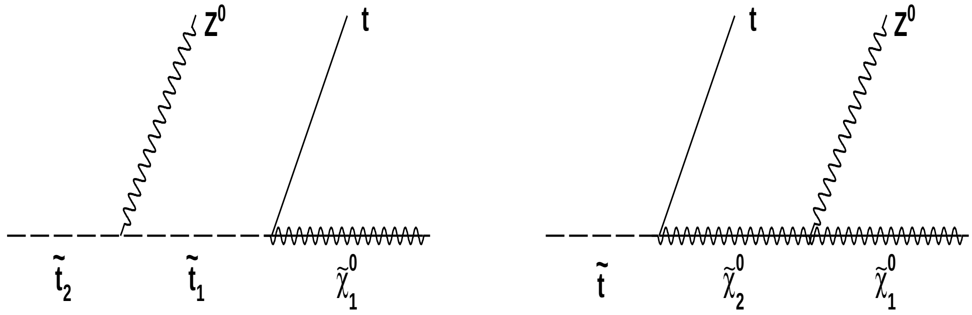

Figure 1: (a) The decay chain of the golden region and (b) an alternative decay chain.

Recently, Perelstein and Spethmann investigated the 'golden region' in the MSSM parameter space, where the amount of fine-tuning is minimized while expermental constraints are satisfied [1]. The decay of a heavier stop into a lighter stop and a Z boson, $\tilde{t}_2 \to \tilde{t}_1 Z$, is kinematically allowed through the golden region. For instance, a benchmark point of the golden region in ref. [1] provides stop masses, $m_{\tilde{t}_2} = 700\,\mathrm{GeV}$, $m_{\tilde{t}_1} = 400\,\mathrm{GeV}$ with branching ratio $B(\tilde{t}_2 \to \tilde{t}_1 Z) = 31\%$. Then, the cascade decay in figure 1 (a) provides a characteristic signature of the golden region scenario at the LHC. However, the interpretation of the golden region signature can be obscured by other types of cascade decays such as the one in figure 1 (b) involving the neutralino decay $\tilde{\chi}_2^0 \to \tilde{\chi}_1^0 Z$, which is realized in different MSSM scenarios but produces the same final state particles as the chain in figure 1 (a). In this note, we show that one way of distinguishing the two confusing decay chains in figure 1, is to investigate Z boson polarization in the decay chains.

For the stop decay $\tilde{t}_2(p) \to \tilde{t}_1(q) + Z(k, \lambda)$, where p, q and k denote 4-momenta of the particles, and $\lambda = \pm 1, 0$ indicate the helicities of Z boson, the matrix element is given by

$$\mathcal{M} \propto (p+q)^\mu \epsilon_\mu^*(k, \lambda). \tag{1}$$

For transverse polarizaion vectors $\epsilon(k, \lambda)$ of Z boson, we have $p \cdot \epsilon(k, \pm 1) = q \cdot \epsilon(k, \pm 1) = 0$ in the rest frame of the decaying stop $\tilde{t}_2$, so that transverse Z polarization does not appear but only longitudinally polarized Z boson is produced from the stop decay in the rest frame. In the laboratory frame where $\tilde{t}_2$ has non-zero spatial momentum, transverse Z polarization is developed through the so-called Wigner rotation [2] even though it is absent in the stop rest frame. However, because of the large hierarchy between stop mass difference and Z boson mass for the golden region scenario, the Wigner rotation effect is so negligible that the Z boson from the stop decay in the laboratory frame is still dominantly longitudinal.

On the other hand, both of transverse and longitudinal Z polarizations are available in $\tilde{\chi}_2^0 \to \tilde{\chi}_1^0 + Z(\lambda)$ decay processes. In the rest frame of decaying neutralino, the relevant decay rates are given by [3]

$$\Gamma[\tilde{\chi}_2^0 \to \tilde{\chi}_1^0 + Z(\pm 1)] \propto m_2^2 + m_1^2 - m_Z^2 - 2 m_2 m_1 \mathcal{A}_\mathcal{N}, \tag{2}$$

$$\Gamma[\tilde{\chi}_2^0 \to \tilde{\chi}_1^0 + Z(0)] \propto m_2^2 + m_1^2 - m_Z^2 - 2 m_2 m_1 \mathcal{A}_\mathcal{N} + \frac{\lambda_Z}{m_Z^2}, \tag{3}$$

JHEP12(2008)074

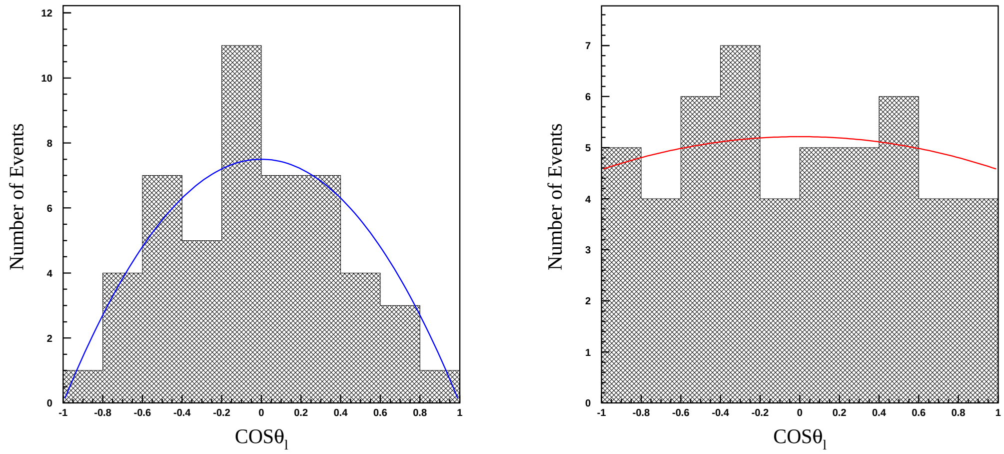

Figure 2: The lepton angular distributions in the Z rest frame with respect to Z polarization direction for (a) the stop decay $\tilde{t}_2 \to \tilde{t}_1 + Z$ and (b) the neutralino decay $\tilde{\chi}_2^0 \to \tilde{\chi}_1^0 + Z$, respectively. 50 Monte Carlo events are used for the distributions.

where m_1 and m_2 are the masses of $\tilde{\chi}_1^0$ and $\tilde{\chi}_2^0$ respectively, $\lambda_Z \equiv [(m_2+m_1)^2 - m_Z^2][(m_2 - m_1)^2 - m_Z^2]$ and $\mathcal{A}_{\mathcal{N}} \equiv (|V|^2 - |A|^2)/(|V|^2 + |A|^2)$. And the vector and axial vector couplings V and A of the Z boson to the neutralino currents are expressed in terms of the neutralino mixing matrix elements [4]. Although the relative production rates of longitudinal and transverse Z polarizations in the $\tilde{\chi}_2^0 \to \tilde{\chi}_1^0 + Z$ decay depend on the neutralino mass spectrum, the $\tilde{\chi}_2^0\tilde{\chi}_1^0 Z$ couplings and the $\tilde{\chi}_2^0$ momentum, they are expected to be similar in magnitude unless $m_2 - m_1$ is too large compared to m_Z.

The Z polarization can be reconstructed through lepton angular distribution in leptonic Z decays $Z \to l^+l^-$ [3]. Figure 2 (a) shows the leptonic angular distribution of $Z \to l^+l^-$ decay in the Z rest frame with respect to the Z polarization direction, where Z bosons come from $\tilde{t}_2 \to \tilde{t}_1 + Z$ decays in the golden region scenario. On the figure, the histogram corresponds to the result of a parton-level Monte Carlo simulation with HERWIG event generator [5], while the solid line to the theoretical expectation which ignore the Wigner rotation effect. Here, 50 Monte Carlo events are used for the histogram. The number of events are expected for the benchmark point in ref. [1] with 300 fb^{-1} luminosity if suitable event selection cuts are imposed. (See ref. [1] for the details.) However notice that, in this work, detector responce and event selection cuts are not included.

On the other hand, the corresponding lepton angular distribution for the case where Z is produced from neutralino decay of $\tilde{\chi}_2^0 \to \tilde{\chi}_1^0 + Z$, is shown in figure 2 (b). Here, as a specific numerical example, we set the neutralino masses as $m_{\tilde{\chi}_2^0} = 221.6\,\mathrm{GeV}$ and $m_{\tilde{\chi}_1^0} = 118.5\,\mathrm{GeV}$ and assume that the neutralino mixing matrix is real. Again, on the figure, the histogram corresponds to 50 Monte Carlo events and the solid line to theoretical expectation without the Wigner rotation effect.

The two decay chains in figure 1 exhibit very distinctive lepton angular distributions in our examples, so that they can be clearly distinguished experimentally, even though more

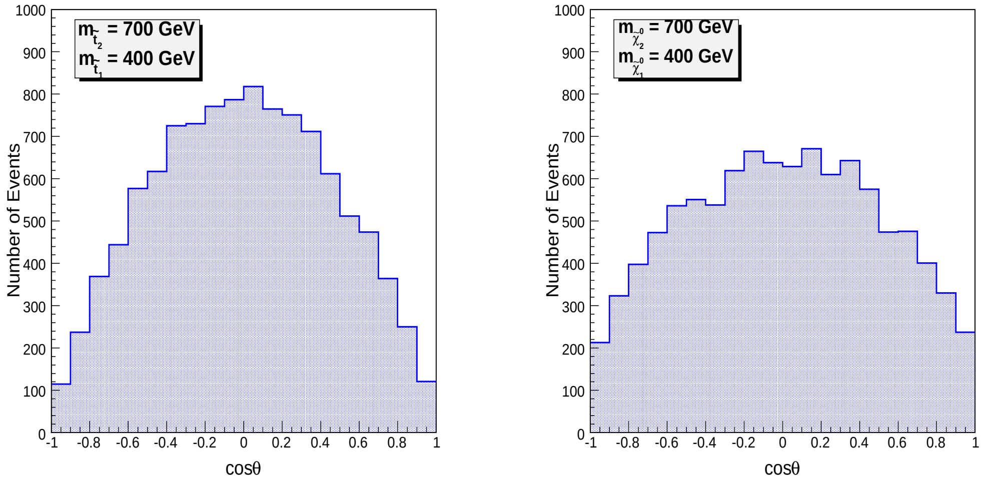

Figure 3: The lepton angular distributions in the Z rest frame with respect to Z polarization direction for (a) the stop decay $\tilde{t}_2 \to \tilde{t}_1 + Z$ and (b) the neutralino decay $\tilde{\chi}_2^0 \to \tilde{\chi}_1^0 + Z$, respectively. Here, we set $m_{\tilde{t}_2} = m_{\tilde{\chi}_2^0} = 700\,\text{GeV}$ and $m_{\tilde{t}_1} = m_{\tilde{\chi}_1^0} = 400\,\text{GeV}$.

careful studies including detector responce, event selection cuts and the SM background would need to be performed.

However, in the examples of figure 2, the masses of mother and daughter particles are very different between the two decay chains. In order to see the effects of spin assignments beside mass spectra, we now compare the two decay chains with matching masses. Figure 3 (a) and (b) show the leptonic angular distributions for the stop decay and the neutralino decay, respectively, in which $m_{\tilde{t}_2} = m_{\tilde{\chi}_2^0} = 700\,\text{GeV}$ and $m_{\tilde{t}_1} = m_{\tilde{\chi}_1^0} = 400\,\text{GeV}$. Here, for a clear comparison, we generated enough number of Monte Carlo events. With such a large mass difference of neutralinos ($m_{\tilde{\chi}_2^0} - m_{\tilde{\chi}_1^0} = 300\,\text{GeV}$), Z polarization becomes dominantly longitudinal ($\sim 84\,\%$). Therefore, figure 3 (b) for the neutralino decay now looks alike figure 3 (a) for the stop decay. Despite of their resemblance, however, they should be distinguishable from each other with enough statistics.

Now let us consider another examples, in which mass differences of mother and daughter particles are not so different from Z boson mass, *e.g.*, $m_{\tilde{t}_2} = m_{\tilde{\chi}_2^0} = 700\,\text{GeV}$ and $m_{\tilde{t}_1} = m_{\tilde{\chi}_1^0} = 600\,\text{GeV}$. The corresponding leptonic angular distributions are shown in figure 4 (a) and (b), for the stop decay and the neutralino decay, respectively. For such a small mass difference of stop particles, the Wigner rotation effect is so significant that transeverse component of Z polarization is largely developed in the laboratory frame, even though it is absent in the rest frame of the decaying stop particle, in the $\tilde{t}_2 \to \tilde{t}_1 + Z$ decay. Therefore, figure 4 (a) shows rather flat angular distribution. On the other hand, for the neutralino decay, the contributions from longitudinal and transverse Z polarization remain similar to each other even after reshuffling of the Z polarization through the Wigner rotation effect, leading to the flat distribution in figure 4 (b). Though figure 4 (a) and (b) are not so different from each other, they should be distinguishable with large statistics.

JHEP12(2008)074

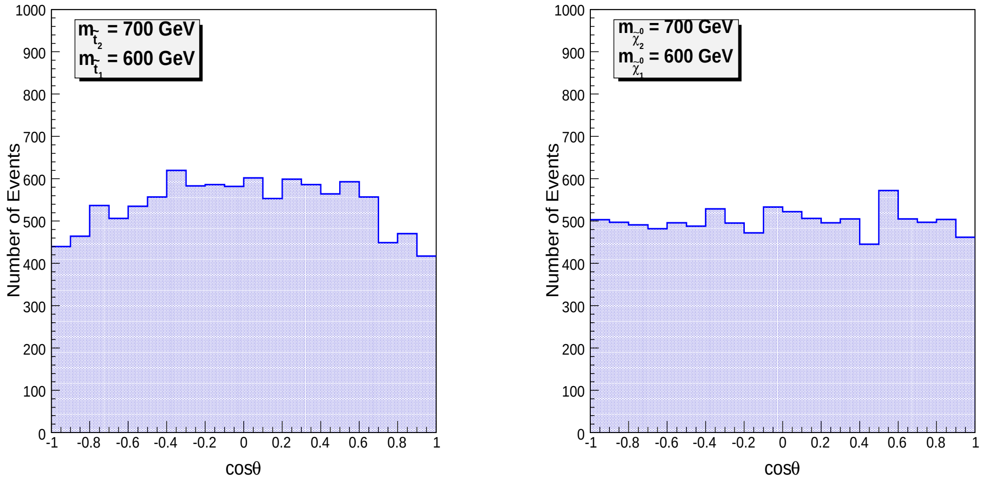

Figure 4: The lepton angular distributions in the Z rest frame with respect to Z polarization direction for (a) the stop decay $\tilde{t}_2 \to \tilde{t}_1 + Z$ and (b) the neutralino decay $\tilde{\chi}^0_2 \to \tilde{\chi}^0_1 + Z$, respectively. Here, we set $m_{\tilde{t}_2} = m_{\tilde{\chi}^0_2} = 700\,\mathrm{GeV}$ and $m_{\tilde{t}_1} = m_{\tilde{\chi}^0_1} = 600\,\mathrm{GeV}$.

Within a given decay chain, Z polarization can also serve as an indicator of the mass difference of mother and daughter particles, *i.e.*, $m_{\tilde{t}_2} - m_{\tilde{t}_1}$ in $\tilde{t}_2 \to \tilde{t}_1 Z$ decay or $m_{\tilde{\chi}^0_2} - m_{\tilde{\chi}^0_1}$ in $\tilde{\chi}^0_2 \to \tilde{\chi}^0_1 Z$ decay, as the Z polarization (and so the leptonic angular distribution) in the laboratory frame depends on the mass difference.

In summary, we showed that Z polarization is useful to discriminate the signal decay chain of the golden region scenario which involves the stop decay $\tilde{t}_2 \to \tilde{t}_1 Z$, from other decay chains including the neutralino decay $\tilde{\chi}^0_2 \to \tilde{\chi}^0_1 Z$ in different MSSM scenarios. Within a given decay chain, Z polarization can also serve as an indicator of the mass difference of mother and daughter particles.

Acknowledgments

We thank S.Y. Choi for his valuable comments on the manuscript. This work was supported by the Korea Research Foundation Grant funded by the Korean Government (MOEHRD, Basic Research Promotion Fund) (KRF-2005-210-C000006), the Center for High Energy Physics of Kyungpook National University, and the BK21 program of Ministry of Education.

References

[1] M. Perelstein and C. Spethmann, *A collider signature of the supersymmetric golden region*, *JHEP* **04** (2007) 070 [hep-ph/0702038].

[2] E.P. Wigner, *On unitary representations of the inhomogeneous lorentz group*, *Ann. Math.* **40** (1939) 149.

[3] S.Y. Choi and Y.G. Kim, *Analysis of the neutralino system in two-body decays of neutralinos*, *Phys. Rev.* **D 69** (2004) 015011 [hep-ph/0311037].

[4] S.Y. Choi, J. Kalinowski, G.A. Moortgat-Pick and P.M. Zerwas, *Analysis of the neutralino system in supersymmetric theories*, *Eur. Phys. J.* **C 22** (2001) 563 [hep-ph/0108117]; *Analysis of the neutralino system in supersymmetric theories*, *Eur. Phys. J.* **C 23** (2002) 769; J. Kalinowsi, *CP-violation in the neutralino system*, *Acta Phys. Polon.* **B34** (2003) 3441 [hep-ph/0306272].

[5] M. Bahr et al., *HERWIG++ physics and manual*, *Eur. Phys. J.* **C 58** (2008) 639 [arXiv:0803.0883].